Targeting the protein prenyltransferases efficiently reduces tumor development in mice with K-RAS-induced lung cancer

Meng Liu[a,b,1], Anna-Karin M. Sjogren[a,1], Christin Karlsson[a], Mohamed X. Ibrahim[a], Karin M. E. Andersson[a], Frida J. Olofsson[a], Annika M. Wahlstrom[a], Martin Dalin[a], Huiming Yu[b], Zhenggang Chen[a,b], Shao H. Yang[c], Stephen G. Young[c], and Martin O. Bergo[a,2]

[a]Wallenberg Laboratory, Institute of Medicine, Sahlgrenska University Hospital, S-41345 Gothenburg, Sweden; [b]Department of Neurosurgery, Qilu Hospital, Shandong University, Jinan 250012, China; and [c]Departments of Medicine and Human Genetics, David Geffen School of Medicine, University of California, Los Angeles, CA 90095

RAS and RHO proteins, which contribute to tumorigenesis and metastasis, undergo posttranslational modification with an isoprenyl lipid by protein farnesyltransferase (FTase) or protein geranylgeranyltransferase-I (GGTase-I). Inhibitors of FTase and GGTase-I were developed to block RAS-induced malignancies, but their utility has been difficult to evaluate because of off-target effects, drug resistance, and toxicity. Moreover, the impact of FTase deficiency and combined FTase/GGTase-I deficiency has not been evaluated with genetic approaches. We found that inactivation of FTase eliminated farnesylation of HDJ2 and H-RAS, prevented H-RAS targeting to the plasma membrane, and blocked proliferation of primary and K-RAS^{G12D}-expressing fibroblasts. FTase inactivation in mice with K-RAS-induced lung cancer reduced tumor growth and improved survival, similar to results obtained previously with inactivation of GGTase-I. Simultaneous inactivation of FTase and GGTase-I markedly reduced lung tumors and improved survival without apparent pulmonary toxicity. These data shed light on the biochemical and therapeutic importance of FTase and suggest that simultaneous inhibition of FTase and GGTase-I could be useful in cancer therapeutics.

mouse models | non-small-cell lung cancer | protein farnesyltransferase | protein geranylgeranyltransferase type I

Many intracellular proteins, such as the RAS and RHO family proteins, are posttranslationally lipidated at a carboxyl-terminal *CAAX* motif. This process is called isoprenylation and is carried out by a pair of cytosolic enzymes, protein farnesyltransferase (FTase) and protein geranylgeranyltransferase type I (GGTase-I) (1). FTase and GGTase-I share a common α-subunit but have unique β-subunits that determine substrate specificity (2, 3). Some *CAAX* proteins, such as H-RAS, HDJ2, and prelamin A, are substrates for FTase, whereas others, such as RAP1A and RHOA, are substrates for GGTase-I (3). Protein isoprenylation facilitates membrane interactions, promotes protein–protein interactions, and can affect protein turnover (4).

The RAS proteins, by far the most thoroughly studied *CAAX* proteins, are involved in the pathogenesis of many forms of cancer (5). Because isoprenylation is essential for the plasma membrane targeting of the RAS proteins and their ability to transform cells (4), FTase inhibitors (FTIs) have been developed and tested as anticancer agents (6). FTIs showed efficacy in preclinical studies of malignancies, including those without RAS mutations (7–9). However, clinical trials of FTIs in humans have not been particularly successful (6). The mechanism by which FTIs inhibit cell growth is not entirely clear, but it likely involves interfering with the farnesylation of several *CAAX* proteins, in addition to RAS (6, 10, 11). Also, different FTIs have different properties (12–15), complicating efforts to define compound- versus mechanism-related effects.

A few years ago, Mijimolle et al. (16) attempted to address the functional relevance of FTase by generating mice with a conditional knockout allele for the gene encoding the β-subunit of FTase (*Fntb*). Cre-mediated recombination appeared to inhibit the farnesylation of HDJ2 and H-RAS, but only partially, and, most remarkably, H-RAS remained in the membrane fraction of cells. They also reported that *Fntb*-deficient fibroblasts grew in culture and that the development of K-RAS-induced tumors was unaffected by *Fntb* deficiency. These findings were surprising for several reasons. First, FTI treatment studies had suggested that the membrane association of H-RAS is utterly dependent on protein farnesylation (17). Second, a nonprenylated mutant of H-RAS (C186S) is found exclusively in the soluble, cytosolic fraction of cells (18). Third, FTI treatment of cells typically results in cell-cycle arrest (19, 20). Fourth, in mouse models, FTIs are efficacious against many tumors, including those without RAS mutations (9, 21).

A potential explanation for the differences between the genetic and pharmacologic studies is that FTIs might affect other proteins aside from FTase. Another is that the *Fntb* knockout allele generated by Mijimolle et al. (16) yielded a transcript with an in-frame deletion (22), and it is conceivable that this mutant transcript yielded a protein with some residual enzymatic activity.

In FTI-treated cells, K-RAS and N-RAS are alternately prenylated by GGTase-I (23–25). That finding prompted both pharmaceutical companies and academic laboratories to develop GGTase-I inhibitors (GGTIs) (26), which have shown promise in preclinical studies (27–31). The rationale for inhibiting GGTase-I is supported by genetic studies in mice: Inactivating the gene for the β-subunit of GGTase-I (*Pggt1b*) reduced tumor formation and prolonged survival in mice with K-RAS-induced lung cancer (32).

Because neither an FTI alone nor a GGTI alone inhibits the prenylation of K- and N-RAS, FTI/GGTI combinations and dual-prenylation inhibitors (DPIs) were developed (33, 34). DPIs and FTI/GGTI combinations block K-RAS prenylation in vivo, but only at high doses that are toxic in mice. However, some studies with FTI/GGTI combinations did not report significant toxicity (27, 35). Thus far, no one has used genetic approaches to study dual inhibition of FTase and GGTase-I.

In this study, we created a conditional knockout allele for *Fntb* and reevaluated the impact of *Fntb* deficiency on protein isoprenylation, cell proliferation, and the growth of K-RAS-induced tumors. We also bred mice homozygous for conditional knockout alleles in both *Fntb* and *Pggt1b* and assessed the effect of combined FTase/GGTase-I deficiency on the development of K-RAS-induced lung cancer.

MEDICAL SCIENCES

Results

Generation and Validation of a Conditional FTase Knockout Allele. To create a conditional knockout allele ($Fntb^{fl}$) for the β-subunit of FTase, we introduced *loxP* sites 1 kb upstream and 1 kb downstream of exon 1 (Fig. 1*A*). Mice homozygous for the conditional allele ($Fntb^{fl/fl}$) were healthy and fertile. $Fntb^{fl/fl}$ mice were bred first with EIIa-*Cre* mice (36) to remove a floxed *neo* cassette and then with deleter-*Cre* mice (37) to produce mice harboring one conditional knockout allele and one knockout allele ($Fntb^{fl/\Delta}$). Primary fibroblasts were cultured from E13.5 $Fntb^{fl/fl}$ embryos. When these cells were incubated with *Cre*-adenovirus (*adCre*), they were converted to $Fntb^{\Delta/\Delta}$ derivatives that had no detectable *Fntb* expression (Fig. 1*B*).

To assess the impact of *Fntb* deficiency on the isoprenylation of FTase substrates, we performed western blots of lysates from β-gal adenovirus- (*adβgal*) and *adCre*-treated $Fntb^{fl/\Delta}$ fibroblasts and control fibroblasts ($Fntb^{fl/+}$). HDJ2 and H-RAS in extracts of *adCre*-treated $Fntb^{fl/\Delta}$ cells exhibited reduced electrophoretic mobilities (Fig. 1*C*), characteristic of the nonfarnesylated forms of these proteins. The absolute levels of HDJ2 did not change, but the levels of H-RAS in *adCre*-treated $Fntb^{fl/\Delta}$ cells were 2- to 4-fold higher than in control cells, as judged by densitometry (Fig. 1*C*).

The electrophoretic mobilities of K-RAS and N-RAS were unchanged, likely because these proteins are isoprenylated by GGTase-I (23–25). HDJ2 and H-RAS accumulated in the cytosolic fraction of $Fntb^{\Delta/\Delta}$ cells, whereas K- and N-RAS remained associated with the membrane fraction (Fig. 1*D*). Inactivating a single *Fntb* allele in $Fntb^{fl/+}$ fibroblasts with *adCre* did not affect the electrophoretic mobilities or the membrane/cytosolic partitioning of HDJ2 and H-RAS (Fig. 1 *C* and *D*).

To determine whether K-RAS and N-RAS are geranylgeranylated in $Fntb^{\Delta/\Delta}$ cells, we isolated $Fntb^{fl/fl}Pggt1b^{fl/fl}$ fibroblasts and treated them with *adCre* to inactivate both *Fntb* and *Pggt1b* ($Fntb^{\Delta/\Delta}Pggt1b^{\Delta/\Delta}$). In $Fntb^{\Delta/\Delta}Pggt1b^{\Delta/\Delta}$ cells, a substantial proportion of K-RAS accumulated in the cytosolic fraction and exhibited a reduced electrophoretic mobility (Fig. 1*E*). A similar shift in the mobility of N-RAS was observed in $Fntb^{\Delta/\Delta}$ cells treated with a GGTI (Fig. 1*F*). $Fntb^{\Delta/\Delta}Pggt1b^{\Delta/\Delta}$ cells remained viable for a few days, but they underwent apoptosis and died within 4 days (Fig. S1 *A* and *B*). Inactivating *Fntb* and *Pggt1b* in cells expressing oncogenic H-RAS targeted to the plasma membrane by an amino-terminal myristoylation sequence also underwent apoptosis (Fig. S1 *C* and *D*).

Fntb Deficiency Blocks Proliferation of Primary and K-RAS^{G12D}-Expressing Fibroblasts. Inactivating a single *Fntb* allele in $Fntb^{fl/+}$ fibroblasts with *adCre* did not affect cell proliferation (Fig. 2*A*). However, inactivating both alleles by treating primary $Fntb^{fl/\Delta}$ fibroblasts with *adCre* dramatically reduced proliferation (Fig. 2*A*). Similar results were found with primary and immortalized $Fntb^{fl/fl}$ cells. Genotypically confirmed $Fntb^{\Delta/\Delta}$ fibroblasts were large and flat and accumulated in the G$_2$M phase of the cell cycle (Fig. 2 *B* and *C*), but the number of apoptotic cells was low (Fig. S1*A*). Inactivating *Fntb* in primary fibroblasts increased p21^{CIP1} levels and delayed serum-stimulated phosphorylation of AKT but did not affect levels of phosphorylated MEK and ERK1/2 (Fig. S2).

When *adCre*-treated $Fntb^{fl/fl}$ cells were left on the culture plates for more than a week, cell growth gradually resumed. However, this growth was due to overgrowth by $Fntb^{fl/\Delta}$ cells (rather than $Fntb^{\Delta/\Delta}$ cells) (Fig. 2*D*). Despite extensive efforts, we were unable to clone $Fntb^{\Delta/\Delta}$ fibroblasts from *adCre*-treated $Fntb^{fl/fl}$ cells. In more than 12 independent experiments, cell growth late after *adCre* treatment was invariably due to overgrowth by $Fntb^{fl/\Delta}$ cells (Fig. 2*E*). In contrast, we had no difficulty in obtaining stable $Fntb^{\Delta/+}$ cell lines after treating $Fntb^{fl/+}$ cells with *adCre* (Fig. 2*E*).

To assess the impact of *Fntb* deficiency on the proliferation of cells expressing K-RAS^{G12D}, we isolated primary fibroblasts from $Fntb^{fl/\Delta}$ and $Fntb^{fl/+}$ embryos harboring an inducible oncogenic K-RAS allele (K^{LSL}) (38). The K^{LSL} allele is normally silent but K-RAS^{G12D} expression can be induced with *Cre*. Incubation of $Fntb^{fl/+}K^{LSL}$ fibroblasts with *adCre* yielded $Fntb^{\Delta/+}K^{G12D}$ cells that proliferated more rapidly (Fig. 2*F*). In contrast, *adCre* treatment of $Fntb^{fl/\Delta}K^{LSL}$ cells (producing $Fntb^{\Delta/\Delta}K^{G12D}$ cells) resulted in G$_2$M cell-cycle arrest (Fig. 2 *F* and *G*).

Inactivating _Fntb_ Increases Survival of Mice with K-RAS-Induced Lung Cancer. To determine the effect of an *Fntb* knockout on the development of a K-RAS-induced malignancy, we bred mice carrying the K^{LSL} allele (*K*) and a lysozyme M-*Cre* allele (*L*) on $Fntb^{fl/\Delta}$ and $Fntb^{fl/+}$ backgrounds (mice harboring both alleles were designated *KL*). Littermate $Fntb^{fl/\Delta}L$ mice were monitored to assess the impact of *Fntb* deficiency in the absence of K-RAS-induced tumors; $Fntb^{fl/+}L$, $Fntb^{fl/+}K$, and $Fntb^{fl/\Delta}K$ mice were used as healthy controls (*Ctr* mice).

We previously showed that *KL* mice express K-RAS^{G12D} in most or all type II pneumocytes and develop lung cancer that is fatal by 25 days of age. Lung weight is increased ~10-fold and alveoli are obliterated by diffuse hyperplasia and adenocarcinoma (32). In keeping with those findings, the maximum survival of $Fntb^{fl/+}KL$ mice was 24 days (Fig. 3*A*). The survival of $Fntb^{fl/\Delta}KL$ mice was
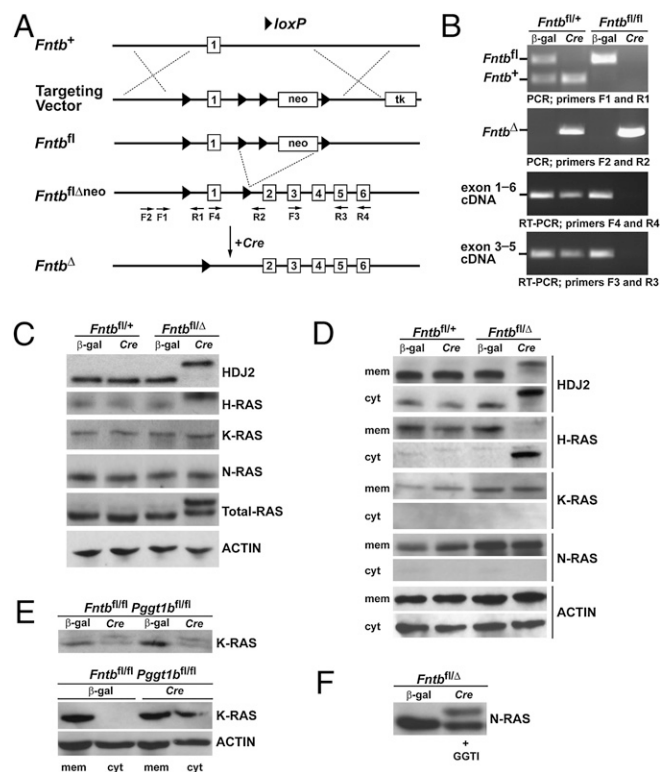

Fig. 1. A conditional knockout allele for the β-subunit of FTase ($Fntb^{fl}$). (*A*) Schematic of the *Fntb* gene-targeting vector. *LoxP* sites were inserted 1 kb upstream and downstream of exon 1. Arrows show the locations of primers for genotyping. *neo*, neomycin-resistance cassette; *tk*, thymidine kinase cassette. (*B*) PCR and RT-PCR analyses demonstrating the inactivation of *Fntb* by treatment with *adCre*. $Fntb^{fl/+}$ and $Fntb^{fl/fl}$ fibroblasts were incubated with *adβgal* or *adCre*, and genomic DNA and total RNA were isolated 4 days later. (*C*) Western blots of extracts from $Fntb^{fl/+}$ and $Fntb^{fl/\Delta}$ fibroblasts incubated with *adβgal* or *adCre*. An antibody against actin was used as a loading control. (*D*) Western blots showing the distribution of proteins in the membrane (mem) and cytosolic (cyt) fractions of *adβgal*- or *adCre*-treated fibroblasts. (*E*) (*Upper*) K-RAS western blot of extracts from $Fntb^{fl/fl}Pggt1b^{fl/fl}$ fibroblasts that had been incubated with *adβgal* or *adCre*. (*Lower*) Western blot showing the distribution of K-RAS in the membrane and cytosolic fractions of $Fntb^{fl/fl}Pggt1b^{fl/fl}$ fibroblasts incubated with *adβgal* or *adCre*. (*F*) N-RAS western blot of $Fntb^{fl/\Delta}$ fibroblasts treated with *adCre* and 10 μM GGTI for 4 days.
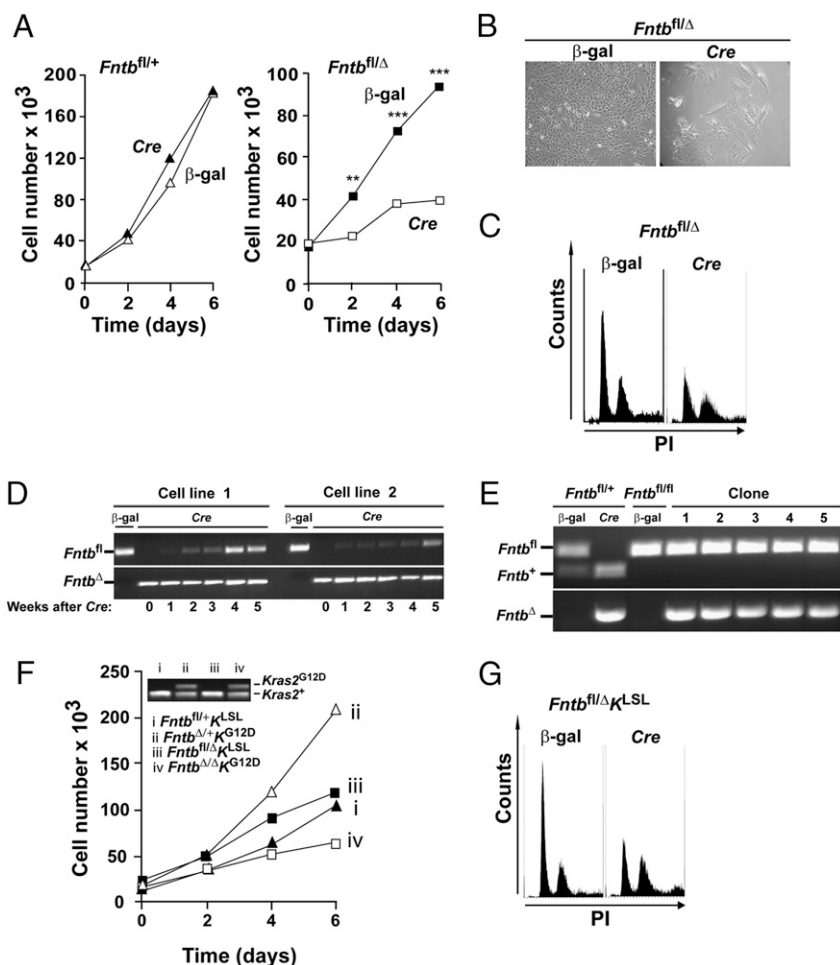
Fig. 2. Inactivating *Fntb* stops fibroblast proliferation. (*A*) Proliferation of *Fntb*$^{fl/+}$ and *Fntb*$^{fl/\Delta}$ primary mouse fibroblasts incubated with *adβgal* or *adCre*. Data show a single cell line assayed in triplicate. Similar results were obtained with two different cell lines of each genotype. **P < 0.01; ***P < 0.001. (*B*) Photomicrographs of *Fntb*$^{fl/\Delta}$ cells incubated with *adβgal* or *adCre*. (*C*) Cell-cycle analysis of *Fntb*$^{fl/\Delta}$ fibroblasts incubated with *adβgal* or *adCre*. PI, propidium iodide. (*D*) PCR genotyping of genomic DNA from *Fntb*$^{fl/fl}$ fibroblasts at various times after incubation with *adβgal* or *adCre*. (*E*) PCR genotyping of genomic DNA from individual clones of *adβgal*- or *adCre*-treated *Fntb*$^{fl/+}$ and *Fntb*$^{fl/fl}$ fibroblasts. (*F*) Proliferation of primary *Fntb*$^{fl/+}K^{LSL}$ and *Fntb*$^{fl/\Delta}K^{LSL}$ fibroblasts incubated with *adβgal* or *adCre*. Data represent the mean of a single cell line/genotype assayed in triplicate. Similar results were obtained in two independent experiments with two cell lines/genotypes. Inset shows PCR genotyping of genomic DNA demonstrating the activation of the K^{G12D} allele in cells incubated with *adCre* (ii and iv) but not in cells incubated with *adβgal* (i and iii). (*G*) Cell-cycle analysis of *adβgal*- and *adCre*-treated *Fntb*$^{fl/\Delta}K^{LSL}$ fibroblasts. The experiment was repeated three times with similar results.

significantly longer, >100 days in some cases (*P* < 0.0001; Fig. 3*A*). The lung weights in 3-week-old *Fntb*$^{fl/\Delta}KL$ mice were lower than in *Fntb*$^{fl/+}KL$ mice (*P* < 0.0001) but higher than in *Fntb*$^{fl/\Delta}L$ mice or *Ctr* mice (Fig. 3*B*). Moreover, histologic analyses revealed nearly complete obliteration of alveoli in *Fntb*$^{fl/+}KL$ lungs, whereas *Fntb*$^{fl/\Delta}KL$ lungs retained areas of normal histology (Fig. 3*C*). Survival, lung weight, and lung histology in *Fntb*$^{fl/\Delta}L$ mice were indistinguishable from those of *Ctr* mice (Fig. 3 *A*–*C*).

PCR genotyping of genomic DNA from *Fntb*$^{fl/\Delta}KL$ lungs revealed activation of the K-RAS^{G12D} allele and a recombined *Fntb* allele (Fig. 3*D*). We harvested protein lysates from lung tissue from 3-week-old *Fntb*$^{fl/+}KL$ and *Fntb*$^{fl/\Delta}KL$ mice and performed western blots with antibodies against the *CAAX* proteins, H-RAS, HDJ2, and prelamin A, which serve as markers of cellular FTase activity (39). In lung extracts of *Fntb*$^{fl/\Delta}KL$ mice, a substantial proportion of H-RAS accumulated in the cytosolic fraction, whereas K-RAS remained in the membrane fraction (Fig. 3*E*). Approximately 50% of the HDJ2 in *Fntb*$^{fl/\Delta}KL$ lungs exhibited a reduced electrophoretic mobility (Fig. 3*F*). Also, reduced FTase activity resulted in an accumulation of nonfarnesylated prelamin A (Fig. 3*F*). There was no difference in levels of phosphorylated ERK1/2 in lung extracts from *Fntb*$^{fl/+}KL$ and *Fntb*$^{fl/\Delta}KL$ lungs (Fig. 3*F*).

Simultaneous Inactivation of *Fntb* and *Pggt1b* Reduces Tumor Load. To assess the effect of combined *Fntb* and *Pggt1b* deficiency on K-RAS-induced tumors, we bred *Fntb*$^{fl/\Delta}Pggt1b$$^{fl/\Delta}KL$ mice and control *KL* mice in which neither prenyltransferase was inactivated. Littermate *Fntb*$^{fl/\Delta}Pggt1b$$^{fl/\Delta}L$ mice were analyzed to determine the impact of *Fntb*/*Pggt1b* deficiency in the absence of K-

RAS-induced tumors. *Fntb*$^{fl/+}Pggt1b$$^{fl/+}L$, *Fntb*$^{fl/\Delta}Pggt1b$$^{fl/+}L$, and *Fntb*$^{fl/+}Pggt1b$$^{fl/\Delta}L$ mice (collectively designated *Ctr*) were used as healthy controls.

Lung weight and histology were indistinguishable in 3-week-old *Fntb*$^{fl/\Delta}Pggt1b$$^{fl/\Delta}KL$ and *Ctr* mice (Fig. 4 *A* and *B*). But in 3-week-old *KL* mice, lung weight was 10-fold higher than in *Ctr* mice (as a result of tumor burden), and the maximum survival was 24 days (Fig. 4 *A*–*C*). The levels of phosphorylated ERK1/2 in lung lysates were lower in *Fntb*$^{fl/\Delta}Pggt1b$$^{fl/\Delta}KL$ mice than in *KL* mice (Fig. 4*D*), as were K_i-67 levels (as judged by immunofluorescence confocal microscopy) (Fig. 4*E*). *Fntb*$^{fl/\Delta}Pggt1b$$^{fl/\Delta}KL$ mice survived far longer than *KL* mice (median, 170 vs. 22 days; *P* < 0.0001) (Fig. 4*C*), but all eventually developed tumors and were euthanized. Lung histology and survival were indistinguishable in *Fntb*$^{fl/\Delta}Pggt1b$$^{fl/\Delta}L$ and *Ctr* mice (Fig. 4 *B* and *C*).

To determine whether farnesylation and geranylgeranylation were inhibited in lungs of *Fntb*$^{fl/\Delta}Pggt1b$$^{fl/\Delta}KL$ mice, we performed western blots on lung lysates from 3-week-old mice. Approximately 25% of HDJ2 exhibited a reduced electrophoretic mobility, characteristic of the nonfarnesylated protein. Protein geranylgeranylation was also inhibited, as the nonprenylated (np) form of RAP1A accumulated in lung lysates (Fig. 5*A*). Moreover, a large proportion of K-RAS accumulated in the cytosolic fraction of lung lysates from *Fntb*$^{fl/\Delta}Pggt1b$$^{fl/\Delta}KL$ mice, suggesting that many cells lacked both FTase and GGTase-I activity (Fig. 5*B*). Immunofluorescence and confocal microscopy revealed prelamin A staining in lung sections from *Fntb*$^{fl/\Delta}KL$ and *Fntb*$^{fl/\Delta}Pggt1b$$^{fl/\Delta}KL$ mice, whereas np-RAP1A staining was detected only in the lungs of *Fntb*$^{fl/\Delta}Pggt1b$$^{fl/\Delta}KL$ mice (Fig. 5*C*). Some cells in lungs from *Fntb*$^{fl/\Delta}Pggt1b$$^{fl/\Delta}KL$ mice exhibited
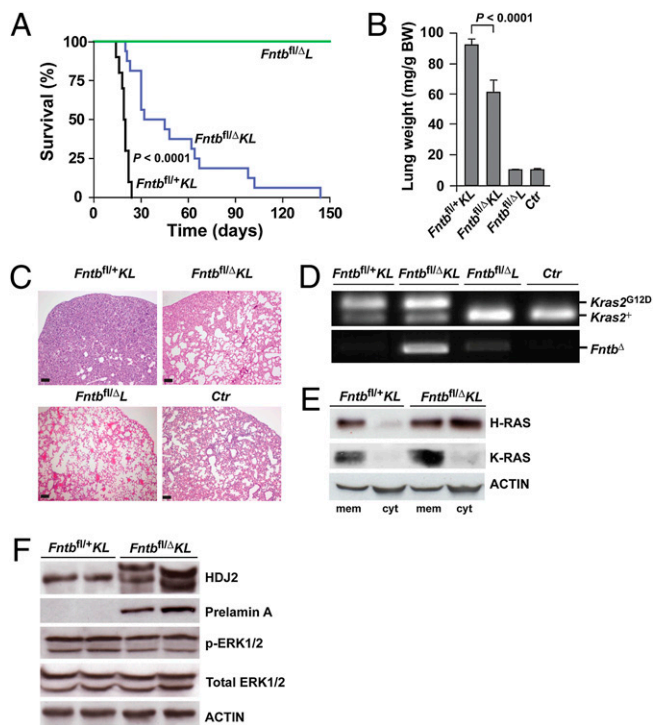
MEDICAL SCIENCES

Fig. 3. Inactivation of *Fntb* reduces tumor development and prolongs survival of mice with K-RAS-induced lung cancer. (*A*) Kaplan–Meier curve showing increased survival in $Fntb^{fl/\Delta}KL$ mice ($n = 16$) compared with $Fntb^{fl/+}KL$ mice ($n = 10$). All $Fntb^{fl/\Delta}L$ mice ($n = 9$) were alive at the end of the experiment (150 days). (*B*) Lung weight in 3-week-old $Fntb^{fl/+}KL$ ($n = 8$), $Fntb^{fl/\Delta}KL$ ($n = 7$), $Fntb^{fl/\Delta}L$ ($n = 6$), and *Ctr* ($n = 5$) mice. (*C*) Hematoxylin/eosin-stained sections of lungs from 3-week-old mice. (Scale bars, 100 μm.) (*D*) Genotyping of wild-type and activated K^{G12D} alleles and the recombined $Fntb^\Delta$ allele by PCR amplification of genomic DNA from lung tissue. (*E*) Western blot showing the distribution of H-RAS and K-RAS in membrane and cytosolic fractions of lung lysates. (*F*) Western blots of protein lysates from the lungs of 3-week-old mice. Actin was used as a loading control.

strong staining for both prelamin A and np-RAP1A (Fig. 5*C* and Fig. S3*A*). These double-positive cells were also identified in lungs of $Fntb^{fl/\Delta}Pggt1b^{fl/\Delta}L$ mice, and some of those cells were type II pneumocytes because they were also positive for SP-C (Fig. S3*B*). Moreover, K-RAS was identified in the cytosolic fraction of lung lysates from $Fntb^{fl/\Delta}Pggt1b^{fl/\Delta}L$ mice (Fig. S3*C*). Despite the presence of cells that apparently lacked both FTase and GGTase-I activity, we found

no evidence of apoptosis in lung sections of $Fntb^{fl/\Delta}Pggt1b^{fl/\Delta}L$ mice (Fig. S4).

In the immunohistochemistry analyses, we detected cells in lungs of $Fntb^{fl/\Delta}Pggt1b^{fl/\Delta}KL$ mice that were positive for np-RAP1A but not prelamin A (Fig. S3*A*) and cells that were negative for both. We suspect that incomplete recombination in the *Fntb* and *Pggt1b* alleles underlies the development of tumors in older $Fntb^{fl/\Delta}Pggt1b^{fl/\Delta}KL$ mice. Indeed, the percentage of genomic DNA with an inactivated *Fntb* allele fell from 18% in 3-week-old mice to 5% in the tumors of 198-day-old mice. Simultaneously, the percent inactivation of the *Pggt1b* gene fell from 20% in 3-week-old mice to 10% in tumors of 198 day-old mice (Fig. 5*D*).

Simultaneous Inactivation of *Fntb* and *Pggt1b* Inhibits Tumorigenesis in a Second K-RAS-Induced Lung Tumor Model. To further investigate how inactivating *Fntb* and *Pggt1b* affects tumor development, we administered *adCre* to $Fntb^{fl/\Delta}Pggt1b^{fl/\Delta}K$ mice, *K* mice heterozygous for one or both of the conditional alleles, and healthy *Ctr* mice (38). *AdCre* results in K^{G12D} expression in a limited number of cells, leading to a limited number of tumors that can be characterized in number, grade, and lesion area. Eight weeks after administration of 5×10^7 pfu *adCre*, *K* mice had large tumors that were easily visible on the surface of the lungs (Fig. 6 *A–C*). However, the lung surface of *adCre*-treated $Fntb^{fl/\Delta}Pggt1b^{fl/\Delta}K$ mice was nearly indistinguishable from that of *Ctr* mice, and $Fntb^{fl/\Delta}Pggt1b^{fl/\Delta}K$ mice had 76% fewer tumors and 79% smaller lesion area than *K* mice (Fig. 6 *A–C*). The lung lesions in *K* mice ranged from atypical adenomatous hyperplasia and epithelial hyperplasia to adenocarcinoma, the most common lesion (identified in 7 of 8 mice; Fig. 6*D*). The lung histology of $Fntb^{fl/\Delta}Pggt1b^{fl/\Delta}K$ mice ranged from entirely normal to the presence of epithelial hyperplasia (Fig. 6*D*) and small adenomas; adenocarcinoma was observed in only 1 of 11 mice.

Discussion

In this study, we produced mice with a conditional knockout allele for *Fntb* and showed that inactivation of *Fntb* eliminated farnesylation of HDJ2 and H-RAS, prevented membrane targeting of H-RAS, and blocked the proliferation of primary, immortalized, and K-RAS^{G12D}-expressing fibroblasts in vitro. Moreover, inactivating *Fntb* in mice with K-RAS-induced lung cancer reduced tumor growth and improved survival. In addition, simultaneous inactivation of *Fntb* and *Pggt1b* had a strong antitumor effect.

Our findings differ significantly from those of Mijimolle et al. (16). In the latter study, the *Fntb* knockout did not affect H-RAS membrane association or stop fibroblast proliferation, nor did it affect the development of K-RAS-induced tumors in mice. When their report was published, it was provocative because it challenged both the
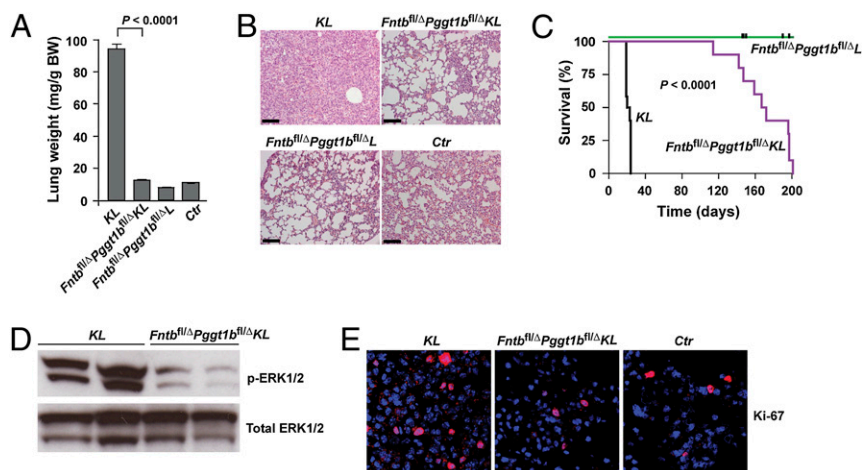

Fig. 4. Simultaneous inactivation of *Fntb* and *Pggt1b* in mice with K-RAS^{G12D}-induced lung cancer. (*A*) Lung weight of 3-week-old *KL* ($n = 4$), $Fntb^{fl/\Delta}Pggt1b^{fl/\Delta}KL$ ($n = 6$), $Fntb^{fl/\Delta}Pggt1b^{fl/\Delta}L$ ($n = 5$), and *Ctr* ($n = 9$) mice. BW, body weight. (*B*) Representative hematoxylin/eosin-stained lung sections of mice from the experiment shown in *A*. (Scale bars, 100 μm.) (*C*) Kaplan–Meier curve showing survival of *KL* ($n = 12$), $Fntb^{fl/\Delta}Pggt1b^{fl/\Delta}KL$ ($n = 10$), and $Fntb^{fl/\Delta}Pggt1b^{fl/\Delta}L$ ($n = 9$) mice. Black tick marks indicate healthy $Fntb^{fl/\Delta}Pggt1b^{fl/\Delta}L$ mice that were euthanized for tissue analyses. (*D*) Western blots of protein extracts from the lungs of 3-week-old *KL* and $Fntb^{fl/\Delta}Pggt1b^{fl/\Delta}KL$ mice showing levels of phosphorylated ERK1/2. Total ERK1/2 was used as a loading control. (*E*) Confocal immunofluorescence micrographs showing expression of K_i-67 (pink) in cells from *KL*, $Fntb^{fl/\Delta}Pggt1b^{fl/\Delta}KL$, and *Ctr* mice. Nuclei were visualized with DAPI (blue).
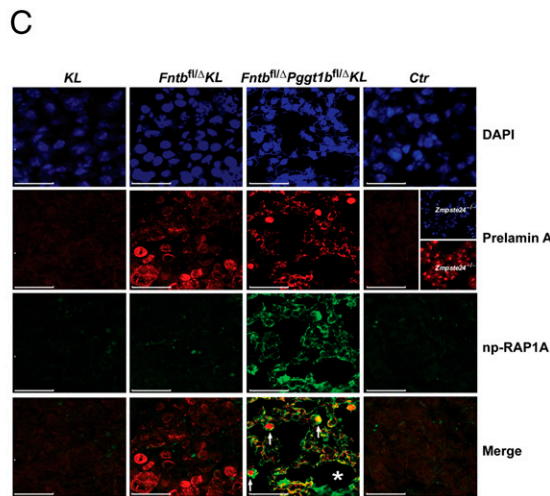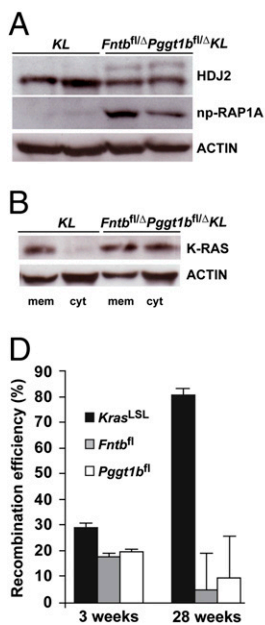
Fig. 5. Reduced FTase and GGTase-I activities in lungs of *Fntb*^{fl/Δ}*Pggt1b*^{fl/Δ}*KL* mice. (*A*) Western blots of protein extracts from lungs of 3-week-old *KL* and *Fntb*^{fl/Δ}*Pggt1b*^{fl/Δ}*KL* mice. Actin was used as a loading control. (*B*) Western blot showing the distribution of K-RAS in the membrane and cytosolic fractions of *KL* and *Fntb*^{fl/Δ}*Pggt1b*^{fl/Δ}*KL* mice. (*C*) Confocal immunofluorescence microscopy showing prelamin A (red) and np-RAP1A (green) expression in lung sections from 3-week-old *KL*, *Fntb*^{fl/Δ}*KL*, *Fntb*^{fl/Δ}*Pggt1b*^{fl/Δ}*KL*, and *Ctr* mice. Nuclei were stained with DAPI (blue). The specificity of prelamin A staining was established with lung sections of *Zmpste24*^{−/−} mice (where prelamin A accumulates due to a defect in the conversion of farnesyl-prelamin A to mature lamin A). Arrows indicate cells positive for both prelamin A and np-RAP1A. Asterisk, alveolus. (Scale bars, 25 μm.) (*D*) Recombination efficiency of the "floxed" *K*^{LSL}, *Fntb*^{fl}, and *Pggt1b*^{fl} alleles determined by quantitative PCR of genomic DNA from lung biopsies of 3-week-old *Fntb*^{fl/Δ}*Pggt1b*^{fl/Δ}*KL* mice (*n* = 5) and from lung tumors of 28-week-old *Fntb*^{fl/Δ}*Pggt1b*^{fl/Δ}*KL* mice (*n* = 2).

widely accepted notion that H-RAS association with membranes depends on protein farnesylation and the view that HDJ2 prenylation depends on FTase. The explanation for the differences between our studies and theirs is unknown; however, we suspect that the differences might relate to the fact that Mijimolle et al.'s allele yielded an unexpected splicing event. Rather than generating a transcript with a nonsense mutation, the mutation yielded a short in-frame deletion in the *Fntb* transcript (22). In contrast, the recombination event in our
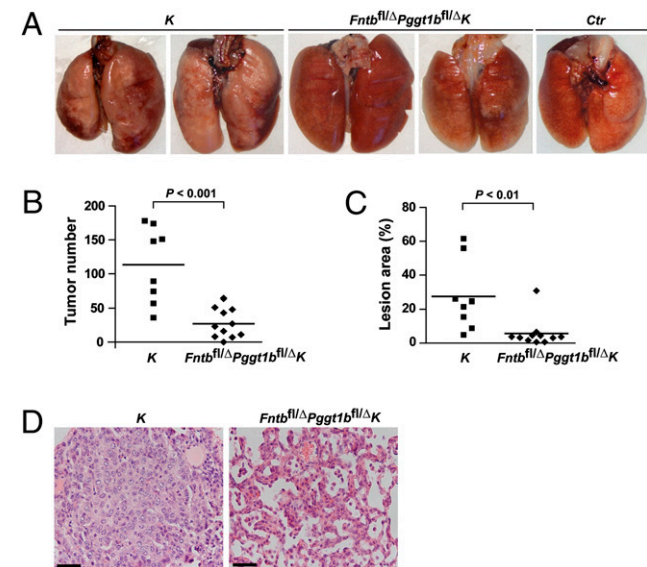

Fig. 6. Inactivation of *Fntb* and *Pggt1b* reduces tumor burden in a second K-RAS^{G12D}-induced lung cancer model. (*A*) Photographs of lungs 8 weeks after inhalation of *adCre*. Note the extensive lesions (white areas) on the surface of lungs from *K* mice and the relatively normal appearance of the lungs from *Fntb*^{fl/Δ}*Pggt1b*^{fl/Δ}*K* mice. (*B* and *C*) Tumor number (*B*) and surface area (*C*) in lungs from *K* (*n* = 8) and *Fntb*^{fl/Δ}*Pggt1b*^{fl/Δ}*K* (*n* = 11) mice 8 weeks after inhalation of *adCre*. (*D*) Hematoxylin/eosin-stained sections of typical lesions in lungs from *K* and *Fntb*^{fl/Δ}*Pggt1b*^{fl/Δ}*K* mice. (Scale bars, 100 μm.)

Fntb allele deleted the promoter and exon 1 and created a bona fide null allele.

Inactivating *Fntb* in fibroblasts induced a G₂M arrest associated with large flattened cells, up-regulated p21^{CIP1}, and reduced serum-stimulated phosphorylation of AKT. Previously, we showed that inactivation of *Pggt1b* induces a G₁ arrest associated with cell rounding and up-regulation of p21^{CIP1}. The cell rounding and cell-cycle arrest could be overcome, at least temporarily, by expressing farnesylated mutants of RHOA and CDC42, suggesting that a limited number of geranylgeranylated proteins are important for those phenotypes. The creation of a bona fide knockout allele for the *Fntb* allele opens the door to performing similar experiments to determine whether geranylgeranylated versions of FTase substrates reverse the phenotypes of *Fntb*-deficient cells.

Fntb deficiency reduced tumor growth and improved survival in mice with K-RAS-induced lung cancer, similar to the effects of inactivating *Pggt1b* (32). Because K-RAS remains prenylated and associated with membranes in both *Fntb*- and *Pggt1b*-deficient cells, these studies support the notion (40) that the therapeutic effects of FTIs and GGTIs are independent of the RAS proteins.

We hypothesized that simultaneous inactivation of *Fntb* and *Pggt1b* would limit tumor growth more effectively than inactivation of either gene alone—in part because this approach would be predicted to inhibit K-RAS prenylation and membrane association. The simultaneous inactivation strategy was effective, at least to an extent, because a substantial proportion of K-RAS in lysates from *Fntb*/*Pggt1b*-deficient fibroblasts, lung tissue, and lung tumors accumulated in the cytosolic fraction. As we predicted, the simultaneous inactivation of *Fntb* and *Pggt1b* had a far greater inhibitory effect on K-RAS-induced tumors than inactivation of either gene alone. However, the main effect of inhibiting FTase and GGTase-I is likely independent of the RAS proteins because both control and myristoylated H-RAS-transfected fibroblasts underwent apoptosis after inactivation of both *Fntb* and *Pggt1b*.

The main concern surrounding the combined inhibition of FTase and GGTase-I has been toxicity (33, 34). Whereas the simultaneous inactivation of *Fntb* and *Pggt1b* clearly induced cell death in fibroblasts, the inactivation of both genes in type II pneumocytes in *Fntb*^{fl/Δ}*Pggt1b*^{fl/Δ}*L* mice did not produce pulmonary disease phenotypes and did not induce apoptosis. Moreover, *Fntb*^{fl/Δ}*Pggt1b*^{fl/Δ}*KL* mice appeared healthy for several months despite widespread expression of K-RAS^{G12D} in the lung. Some

cells in *Fntb*^{fl/Δ}*Pggt1b*^{fl/Δ}*KL* lungs clearly lacked both enzymes, as a large proportion of K-RAS in lung lysates was found in the cytosolic fraction. Also, immunochemical studies revealed that some cells were positive for both prelamin A and np-RAP1A. It is intriguing that some cells in the lung were apparently viable despite the absence of both FTase and GGTase-I. However, our genetic approach does not allow us to address the impact of FTase and GGTase-I deficiency in every lung cell (such as lung stem cells), and we cannot rule out the possibility that a more widespread inactivation of these enzymes would be toxic.

In summary, our findings support the idea that farnesylation is essential for H-RAS membrane association, HDJ2 prenylation, and fibroblast proliferation in vitro. In mice harboring a mutationally activated form of K-RAS in the lung, blocking protein farnesylation retarded tumor growth and improved survival. Our results also support the idea that simultaneous inhibition of FTase and GGTase-I could be therapeutically useful. Finally, the experimental approach described here should be useful for dissecting the in vivo importance of protein farnesylation and geranylgeranylation in other cell types in a variety of diseases.

Materials and Methods

A Conditional Knockout Allele for *Fntb*. A 2.2-kb fragment spanning promoter sequences, exon 1, and parts of intron 1 was amplified by PCR from the genomic DNA of strain 129/OlaHsd embryonic stem (ES) cells. The fragment was cloned into *pNB1*, which contains a polylinker flanked by *loxP* sites. The floxed fragment was excised and cloned into pKS*loxP*NTmod (41) upstream of a floxed *neo* cassette. Finally, 5′- and 3′-flanking arms were amplified by PCR and cloned upstream and downstream, respectively, of the floxed exon 1 fragment and *neo* cassette. The gene-targeting vector was electroporated into 129/OlaHsd ES cells, and targeted clones (identified by Southern blotting with flanking probes) were used to produce germline-transmitting chimeric mice. A detailed description of all other methods appears in *SI Materials and Methods*.

1. Lane KT, Beese LS (2006) Lipid posttranslational modifications. Structural biology of protein farnesyltransferase and geranylgeranyltransferase type I. *J Lipid Res* 47: 681–699.
2. Seabra MC, Reiss Y, Casey PJ, Brown MS, Goldstein JL (1991) Protein farnesyltransferase and geranylgeranyltransferase share a common α subunit. *Cell* 65:429–434.
3. Casey PJ, Seabra MC (1996) Protein prenyltransferases. *J Biol Chem* 271:5289–5292.
4. Kato K, et al. (1992) Isoprenoid addition to Ras protein is the critical modification for its membrane association and transforming activity. *Proc Natl Acad Sci USA* 89:6403–6407.
5. Bos JL (1989) ras oncogenes in human cancer: A review. *Cancer Res* 49:4682–4689.
6. Basso AD, Kirschmeier P, Bishop WR (2006) Lipid posttranslational modifications. Farnesyl transferase inhibitors. *J Lipid Res* 47:15–31.
7. Kohl NE, et al. (1995) Inhibition of farnesyltransferase induces regression of mammary and salivary carcinomas in ras transgenic mice. *Nat Med* 1:792–797.
8. Omer CA, et al. (2000) Mouse mammary tumor virus-Ki-rasB transgenic mice develop mammary carcinomas that can be growth-inhibited by a farnesyl:protein transferase inhibitor. *Cancer Res* 60:2680–2688.
9. Sepp-Lorenzino L, et al. (1995) A peptidomimetic inhibitor of farnesyl:protein transferase blocks the anchorage-dependent and -independent growth of human tumor cell lines. *Cancer Res* 55:5302–5309.
10. Sebti SM, Hamilton AD (2000) Farnesyltransferase and geranylgeranyltransferase I inhibitors and cancer therapy: Lessons from mechanism and bench-to-bedside translational studies. *Oncogene* 19:6584–6593.
11. Sebti SM, Der CJ (2003) Searching for the elusive targets of farnesyltransferase inhibitors. *Nat Rev Cancer* 3:945–951.
12. End DW, et al. (2001) Characterization of the antitumor effects of the selective farnesyl protein transferase inhibitor R115777 in vivo and in vitro. *Cancer Res* 61:131–137.
13. Liu M, et al. (1998) Antitumor activity of SCH 66336, an orally bioavailable tricyclic inhibitor of farnesyl protein transferase, in human tumor xenograft models and wap-ras transgenic mice. *Cancer Res* 58:4947–4956.
14. Rose WC, et al. (2001) Preclinical antitumor activity of BMS-214662, a highly apoptotic and novel farnesyltransferase inhibitor. *Cancer Res* 61:7507–7517.
15. Hunt JT, et al. (2000) Discovery of (*R*)-7-cyano-2,3,4,5-tetrahydro-1-(1*H*-imidazol-4-ylmethyl)-3-(phenylmethyl)-4-(2-thienylsulfonyl)-1*H*-1,4-benzodiazepine (BMS-214662), a farnesyltransferase inhibitor with potent preclinical antitumor activity. *J Med Chem* 43: 3587–3595.
16. Mijimolle N, et al. (2005) Protein farnesyltransferase in embryogenesis, adult homeostasis, and tumor development. *Cancer Cell* 7:313–324.
17. Lerner EC, et al. (1995) Ras CAAX peptidomimetic FTI-277 selectively blocks oncogenic Ras signaling by inducing cytoplasmic accumulation of inactive Ras-Raf complexes. *J Biol Chem* 270:26802–26806.
18. Willumsen BM, Christensen A, Hubbert NL, Papageorge AG, Lowy DR (1984) The p21 ras C-terminus is required for transformation and membrane association. *Nature* 310: 583–586.
19. Ashar HR, et al. (2000) Farnesyl transferase inhibitors block the farnesylation of CENP-E and CENP-F and alter the association of CENP-E with the microtubules. *J Biol Chem* 275:30451–30457.
20. Crespo NC, Ohkanda J, Yen TJ, Hamilton AD, Sebti SM (2001) The farnesyltransferase inhibitor, FTI-2153, blocks bipolar spindle formation and chromosome alignment and causes prometaphase accumulation during mitosis of human lung cancer cells. *J Biol Chem* 276:16161–16167.
21. Nagasu T, Yoshimatsu K, Rowell C, Lewis MD, Garcia AM (1995) Inhibition of human tumor xenograft growth by treatment with the farnesyl transferase inhibitor B956. *Cancer Res* 55:5310–5314.
22. Yang SH, et al. (2009) Caution! Analyze transcripts from conditional knockout alleles. *Transgenic Res* 18:483–489.
23. James G, Goldstein JL, Brown MS (1996) Resistance of K-RasB^{V12} proteins to farnesyltransferase inhibitors in Rat1 cells. *Proc Natl Acad Sci USA* 93:4454–4458.
24. Whyte DB, et al. (1997) K- and N-Ras are geranylgeranylated in cells treated with farnesyl protein transferase inhibitors. *J Biol Chem* 272:14459–14464.
25. Rowell CA, Kowalczyk JJ, Lewis MD, Garcia AM (1997) Direct demonstration of geranylgeranylation and farnesylation of Ki-Ras in vivo. *J Biol Chem* 272:14093–14097.
26. El Oualid F, Cohen LH, van der Marel GA, Overhand M (2006) Inhibitors of protein: Geranylgeranyl transferases. *Curr Med Chem* 13:2385–2427.
27. Sun J, Qian Y, Hamilton AD, Sebti SM (1998) Both farnesyltransferase and geranylgeranyltransferase I inhibitors are required for inhibition of oncogenic K-Ras prenylation but each alone is sufficient to suppress human tumor growth in nude mouse xenografts. *Oncogene* 16:1467–1473.
28. Sun J, et al. (1999) Antitumor efficacy of a novel class of non-thiol-containing peptidomimetic inhibitors of farnesyltransferase and geranylgeranyltransferase I: Combination therapy with the cytotoxic agents cisplatin, Taxol, and gemcitabine. *Cancer Res* 59: 4919–4926.
29. Sun J, et al. (2003) Geranylgeranyltransferase I inhibitor GGTI-2154 induces breast carcinoma apoptosis and tumor regression in H-Ras transgenic mice. *Cancer Res* 63: 8922–8929.
30. Peterson YK, Kelly P, Weinbaum CA, Casey PJ (2006) A novel protein geranylgeranyltransferase-I inhibitor with high potency, selectivity, and cellular activity. *J Biol Chem* 281:12445–12450.
31. Watanabe M, et al. (2008) Inhibitors of protein geranylgeranyltransferase I and Rab geranylgeranyltransferase identified from a library of allenoate-derived compounds. *J Biol Chem* 283:9571–9579.
32. Sjogren A-KM, et al. (2007) GGTase-I deficiency reduces tumor formation and improves survival in mice with K-RAS-induced lung cancer. *J Clin Invest* 117:1294–1304.
33. Lobell RB, et al. (2001) Evaluation of farnesyl:protein transferase and geranylgeranyl: protein transferase inhibitor combinations in preclinical models. *Cancer Res* 61: 8758–8768.
34. deSolms SJ, et al. (2003) Dual protein farnesyltransferase-geranylgeranyltransferase-I inhibitors as potential cancer chemotherapeutic agents. *J Med Chem* 46:2973–2984.
35. Di Paolo A, et al. (2001) Inhibition of protein farnesylation enhances the chemotherapeutic efficacy of the novel geranylgeranyltransferase inhibitor BAL9611 in human colon cancer cells. *Br J Cancer* 84:1535–1543.
36. Lakso M, et al. (1996) Efficient in vivo manipulation of mouse genomic sequences at the zygote stage. *Proc Natl Acad Sci USA* 93:5860–5865.
37. Schwenk F, Baron U, Rajewsky K (1995) A cre-transgenic mouse strain for the ubiquitous deletion of loxP-flanked gene segments including deletion in germ cells. *Nucleic Acids Res* 23:5080–5081.
38. Jackson EL, et al. (2001) Analysis of lung tumor initiation and progression using conditional expression of oncogenic K-ras. *Genes Dev* 15:3243–3248.
39. Adjei AA, et al. (2000) A phase I trial of the farnesyl transferase inhibitor SCH66336: Evidence for biological and clinical activity. *Cancer Res* 60:1871–1877.
40. Lebowitz PF, Prendergast GC (1998) Non-Ras targets of farnesyltransferase inhibitors: Focus on Rho. *Oncogene* 17 (11 Reviews):1439–1445.
41. Hanks M, Wurst W, Anson-Cartwright L, Auerbach AB, Joyner AL (1995) Rescue of the En-1 mutant phenotype by replacement of En-1 with En-2. *Science* 269:679–682.